Modeling Control Strategies for Laminated Root Rot in Managed Douglas-fir Stands: Model Development

W. J. Bloomberg

Research scientist, Pacific Forestry Centre, Canadian Forestry Service, 506 West Burnside Road, Victoria, B.C. V8Z 1M5.
Field plot data for comparison with model results were kindly provided by Dr. Boris Tkacz.
Accepted for publication 22 September 1987.

ABSTRACT

Bloomberg, W. J. 1988. Modeling control strategies for laminated root rot in managed Douglas-fir stands: Model development. Phytopathology 78:403-409.

A model of laminated root rot caused by *Phellinus weirii* was developed to assess potential control strategies in managed Douglas-fir stands. The model mimicked key processes in disease initiation and development quantified as functions of time and space. These processes were horizontal and vertical tree root distribution, root contact with inoculum and among root systems, spread of mycelium through root systems, root decay, reduction of diameter growth in infected trees, tree mortality, and persistence of inoculum in roots of stumps and killed trees. The processes were expressed as mathematical functions which were integrated in a computer program to calculate spread of the disease and stand-growth loss and mortality. Data for quantification of functions were obtained by experiments and from the literature. Simulated control practices included infected stump removal, sanitation fellings, and mixed planting of Douglas-fir and resistant species. Accuracy of the model was tested by comparing calculated disease spread and mortality with the following data: 1) spread and damage in two 60-yr-old, 1-ha stands in Oregon, 2) results from a statistically based model for spread and damage that has performed satisfactorily, and 3) observed spread and damage behavior in stands of different ages and growth rates. Results from the model compared favorably with all of the above situations.

Additional key words: computer simulation, impact.

Laminated root rot of Douglas-fir (*Pseudotsuga menziesii* (Mirb.) Franco), caused by *Phellinus weirii* (Murr.) Gilbertson, is the major source of wood loss on the coastal Douglas-fir zone of British Columbia (5) and one of the most damaging diseases in the Pacific Northwest (6). The disease develops over the entire rotation of second-growth stands (about 100 yr), but only fragmented information is available on the effects of stand age, stand and site conditions, stand history, and silvicultural treatments. The rationale for a modeling approach to research into the disease was to increase understanding of how to manage it over a range of conditions.

No published models of Douglas-fir stand growth that include the effects of root rot are available. A statistically based model of root rot (1) implicitly includes stand and site factors in estimating spread and impact but cannot use explicit values for them, which are essential for evaluating interactions of stand, disease, and management factors. A biologically based model of a stand infected by *P. weirii* would allow these interactions to be examined depending on how accurately the host, pathogen, disease, and silvicultural processes could be quantitatively described.

The model being described is based on statistical relationships for processes wherever available; published measurements of host and pathogen processes, extrapolated where necessary; quantification of published descriptions of disease processes; and computing techniques such as pseudorandomization. The modeling method orders the key processes in tree growth and mortality in a logical sequence so that their interactions can be evaluated numerically. The model allows evaluation of how changes in tree variables, representing silvicultural actions, and disease variables, representing different control procedures, modify the interactions.

The objective was to obtain general estimates of the effects of interactions among stand, site, and silvicultural treatment factors on disease development.

MATERIALS AND METHODS

Model development. Key processes were defined as follows: 1) growth of tree roots, 2) contact between tree and infected stump roots or among tree roots, 3) root infection, 4) spread of mycelium of *P. weirii* in tree roots, 5) reduction of tree growth as a function of root decay, 6) tree mortality, and 7) persistence of viable inoculum of *P. weirii* in roots. Tree variables were number per hectare, growth rate, spatial distribution, and selective felling. Stump variables were number per hectare, sizes and infectivity, spatial pattern, and selective removal.

The model design was "single tree, distance-dependent" (12): individual trees constituted the model units and their spatial coordinates were three-dimensional. Temporal coordinates began at stand establishment, extended to harvest age (100 yr), and were subdivided into 5-yr age classes. Unless otherwise stated, all equations were derived from data collected on medium-quality Douglas-fir sites (10) on southern Vancouver Island. The ordering of the key processes into a coherent model framework is shown in Table 1.

The model is driven by the state of tree root systems; i.e., all consequences flow from properties of individual tree roots. In the shallow, stony soils of coastal British Columbia, the symmetrical pattern of root development in Douglas-fir is obscured early in the life of trees (9) making pattern analysis inappropriate. Therefore, regression analysis of the distribution of root elements in a soil matrix was used to provide the spatial definition of root systems. The matrix comprised equidistant 0.5-m zones concentric on the tree stem-base, further stratified into four cardinal quadrants and 0.25-m depth zones (Fig. 1). Root elements were defined as segments of roots and root branches, to a minimum diameter of 0.5 cm, occurring in each soil matrix cell. Number and sizes of elements in each horizontal or depth cell were calculated as functions of tree diameter at 1.4 m, i.e., diameter at breast height (dbh) (2).

This approach provided fairly reliable ($R^2 > 0.70$) estimates of maximum average horizontal extent of each root system (Table 2, Equation 1), total number of root elements for a tree (Table 2, Equation 2), and number of root elements in each horizontal and vertical soil matrix cell (Table 2, Equations 3 and 4). Variation in the azimuthal distribution of root elements obscured any differences among quadrants; therefore, equal proportions were assigned to each.

Because trees less than 5 yr old (age class 1) were too small to have measurable dbh, the initial values were set such that later dbh growth of uninfected trees replicated that measured in test plots. By setting different initial values, a distribution of dbh classes was obtained that was similar to the distribution in test plots.

For each suscept tree, number of contacts between a root and an infection source was calculated from the aggregate number of root elements in matrix cells within quadrants common to both the root and the infection source (Fig. 2). Infection sources were the infected roots of stumps from the previous stand or of infected trees in the current stand. The number of roots per cubic meter of soil rather than root size was most closely related to probability of contact (14). The contact coefficient was $0.0335/m^3$ soil; i.e., approximately 30 root elements/m^3 resulted in one root contact (Table 2, Equation 5).

Number of root infections per matrix cell arising from contacts was calculated from the joint proportions of healthy root elements of each suscept tree and infected elements of each infection source (Table 2, Equation 6; Fig. 2). A coefficient value of 1.0 was used, denoting that all contacts were assumed to give rise to infections.

TABLE 1. Ordering of key processes in a model of laminated root rot (*Phellinus weirii*) of Douglas-fir

Step	Process	Derivation[a]
1	Assign stump diameters, infection status, and locations.	Variable initializing file
2	Calculate numbers and spatial distribution of stump-root elements.	Equations 1–4
3	Assign tree diameters, resistance status, and locations.	Variable initializing file
4	Calculate numbers and spatial distribution of tree-root elements.	Equations 1–4
5	For each tree, calculate numbers of root elements in soil matrix cells common to each stump and to each neighboring tree.	Soil matrix array
6	Calculate number of root contacts.	Equation 5
7	Calculate mycelial viability and number of infections.	Equations 6 and 11
8	Calculate mycelial spread among tree-root elements.	Equations 7 and 8
9	Calculate reduction in periodic diameter increment and current diameter at breast height (1.4 m).	Equations 9 and 10
10	Calculate tree mortality.	Lethal level of increment reduction
11	Repeat steps 4–10 for age classes 2 and older.	

[a] Equations are described in Table 2.

TABLE 2. Explanation and basis of equations used in modeling laminated root rot (*Phellinus weirii*) of Douglas-fir

Equation No.	Definition of variables	Basis[a]
1	$DIST_{max} = 0.136\ dbh\ R^2 = 0.97$ $DIST_{max}$ is the average horizontal extent of individual roots from the center of the base of a tree in meters; dbh is the tree diameter in centimeters at 1.4 m from ground level.	5
2	$\log TOTNR = 0.9745 + 0.0677\ dbh - 0.00081\ dbh^2\ R^2 = 0.73$ TOTNR is the total number of root elements in all cells.	5
3	$\log (NR_{dist}) = A\ (\log TOTNR) - 0.20\ DIST - 0.10\ R^2 = 0.82$ NR is the number of root elements in soil matrix cells at each 0.5-m distance stratum from a tree stem base; DIST is the distance of the stratum from stem base in 0.5-m units; A is a coefficient for each dbh class ranging from 1.3 for trees 0.1–2.5 cm, to 0.95 for trees >17.6-cm dbh.	5
4	$PR_{depth} = A_{depth} + (B_{depth})\ dbh$ PR_{depth} is the proportion of root elements in soil matrix cells at each 0.25-m depth stratum from a tree stem base; A and B are intercept values and coefficients, respectively, for each depth stratum.	5
5	$NCON = 0.0335\ (NR_s + NR_n)$ NCON is the number of root contacts in a soil matrix cell; NR_s and NR_n are the number of root elements per cubic meter in that cell for the suscept and neighbor trees, respectively.	2
6	$NI = A\ (NCON\ (NR_{s,h}/NR_{s,t})\ (NR_{n,i}/NR_{n,t}))$ NI is the number of infections occurring in a soil matrix cell; NCON is the number of root contacts in the cell; $NR_{s,h}$ and $NR_{s,t}$ are the numbers of suscept tree healthy and total roots, respectively, in the cell; $NR_{n,i}$ and $NR_{n,t}$ are the numbers of neighbor tree infected and total roots, respectively, in the cell. A is a coefficient of infection efficiency.	Combined probability calculation
7	$NC = SR/0.5$ NC is the number of soil matrix cells through which mycelium of *Phellinus weirii* spreads during one age class of the model; SR is the measured spread rate of the fungus in meters per age class in yr.	17
8	$NI_c = NI_c + NS_{c+1,p} + NS_{c-1,d}$ NI_c is the cumulative number of root elements that are infected in a soil matrix cell; $NS_{c+1,p}$ is the number of root elements in the distal cell that are spreading in a proximal direction; $NS_{c-1,p}$ is the number of root elements in the proximal cell that are spreading in a distal direction, given that $NI_c < NR_{s+h}$, the number of root elements available for infection.	Array arithmetic
9	$\log DINCH_{age} = 4.651 - 2.808(\log AGE) + 0.2004(\log AGE^3)\ R^2 = 0.90$ $DINCH_{age}$ is the diameter increment percent at breast height (1.4 m) for healthy trees in a 5-yr age class; AGE is the tree age in years.	Bloomberg (*unpublished*)
10	$DINCI_{age} = DINCH_{age}(0.0171TOTNR - 0.0114INFNR) / 0.0171TOTNR\ R^2 = .73$ $DINCI_{age}$ is the periodic dbh increment percent for infected trees in a 5-yr age class; TOTNR is the total number of root elements and INFNR the number of infected root elements of a tree.	5
11	$VRED = A\ (TM)\ (DIST_c/DIST_{max})$ VRED is the viability reduction percent of *Phellinus weirii* in root elements in a soil matrix cell; TM is the number of age classes elapsed since tree death; $DIST_c$ is the horizontal distance of the cell from the stem base; $DIST_{max}$ is maximum horizontal extent of the root system; A is a coefficient.	7

[a] Literature reference or explanation.

Spread of mycelium distally or proximally from infection points was calculated for root elements in each cell. Spread rate from one cell to another was determined from the measured linear mycelial growth of *P. weirii* along inoculated tree roots (25 cm/yr) (17) and the cell horizontal length (0.5 m, Table 1, Equation 7). The number of root elements to which mycelium spread during each time step was calculated from the direction of mycelium movement in adjacent cells (Table 2, Equation 8).

Proximally spreading mycelium could pass via the root collar to root elements in cells in other quadrants or depth strata (18) (Fig. 3). To allow for the spread of mycelium along a root to its branches, one root element could infect several elements in a proximally adjacent cell. The number of additional elements infected was determined by the ratio of total number of elements in one cell to total number of elements in its distal neighbor. No distinction was made between spread rates of ectotrophic and endotrophic mycelium or among different root diameters. Although endotrophic spread in large-diameter roots appears to be initially slower (17), the lag between endotrophic and ectotrophic mycelial fronts remained approximately the same in older infections regardless of root diameter (3).

The relation of tree growth reduction to disease spread in the root system was estimated from regression analysis of stem-growth variables in 40-yr-old trees (2). The most highly significant relationship was between 5-yr periodic dbh increment percent (periodic dbh increment as a percent of the dbh at the beginning of the period) and the numbers of total and infected roots. In healthy trees, dbh increment percent at ages 5–90 yr was determined from increment borings of 6–12 trees in each of 12 stands (Bloomberg, *unpublished*) (Table 2, Equation 9). Trees selected for boring were in the dominant or codominant crown classes and were in the healthy portions of stands. Cores were taken at dbh horizontally along two radii at right angles passing through the pith. Increments at 5-yr intervals were measured with the aid of a dissecting microscope (× 10). The measurements for the two radii were averaged. Reduction of dbh increment percent in infected trees at ages 5–100 yr was calculated from healthy tree dbh increment percent and the proportionalized reduction for 40-yr-old trees (Table 2, Equation 10; Fig. 4).

Mortality in infected trees was judged to have occurred when dbh growth was reduced to 35% of that expected in the absence of infection. The lethal level was based on results in close agreement from Oregon (15) and southern Vancouver Island stands which included standing dead and wind-thrown infected trees (4).

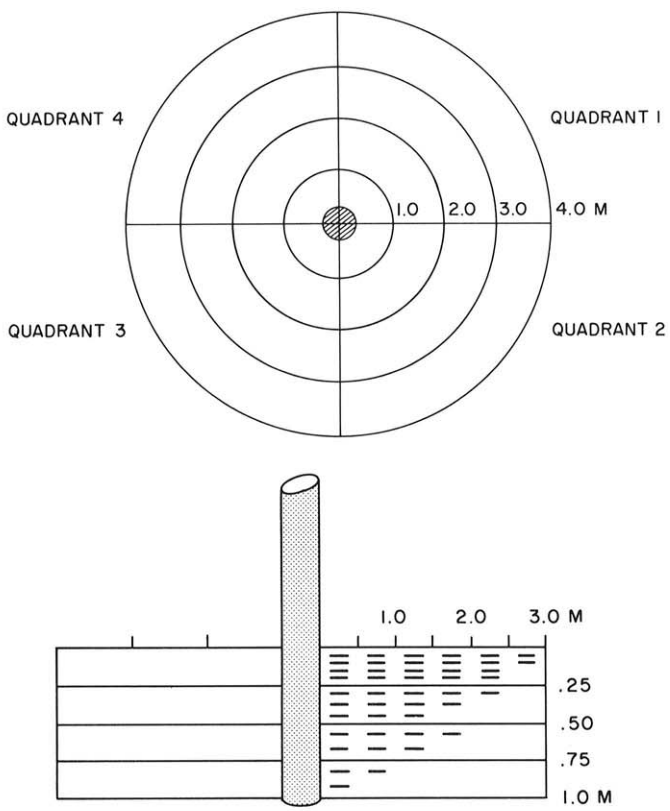

Fig. 1. Soil matrix used to assign spatial distribution of root elements in Douglas-fir. **Top,** Horizontal strata comprised equidistant zones concentric on the tree stem base (hatched circle). **Bottom,** Distribution of root elements horizontally and vertically in a soil matrix. For calculation of numbers of elements in each cell, see Table 2, Equations 1–4.

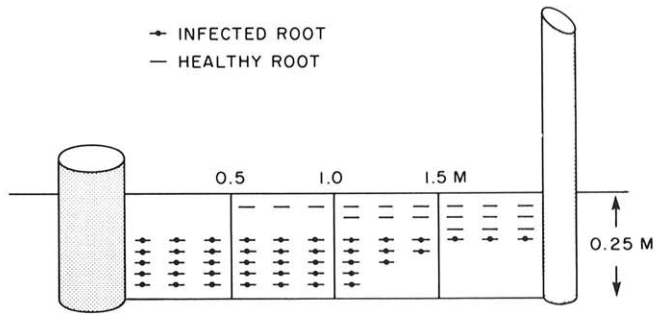

Fig. 2. Root elements of a suscept tree (right) and root elements of an infected stump (left) occupying the same soil matrix cells. − = Suscept root; + = stump root. Number of root contacts in each soil matrix cell was calculated from the aggregate numbers of root elements in a cell. (See Table 2, Equation 5.)

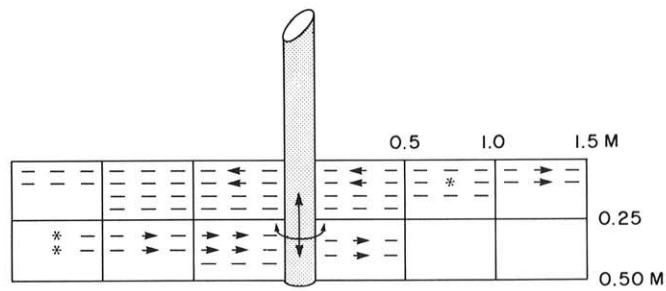

Fig. 3. Spread of mycelium of *Phellinus weirii* from infection points (*) proximally (←) and distally (→) through root system. Vertical and radial spread can occur via the root crown to root elements in other soil matrix cells. For rate and direction of spread, see Table 2, Equations 7 and 8, and text.

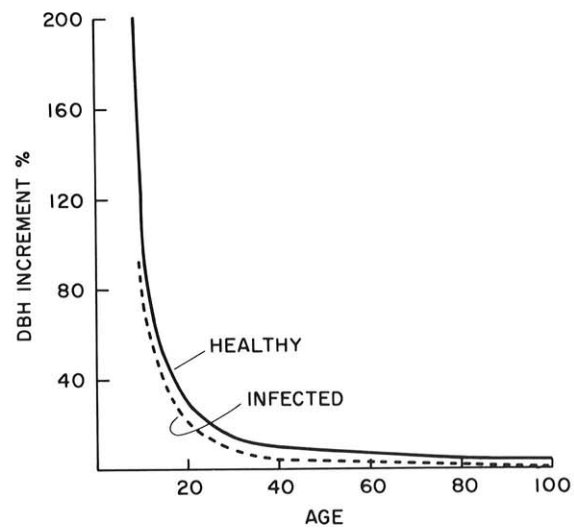

Fig. 4. Relationship of periodic diameter increment percent at breast height (1.4 m) to tree age (yr) in healthy Douglas-fir and Douglas-fir infected by *Phellinus weirii*. For curve equations, see Table 2, Equations 9 and 10.

Tree growth for each 5-yr growth cycle was calculated by applying dbh increment percent to the dbh of the previous age class. The recalculated dbh for the current growth cycle was applied to recalculation of root growth by Equations 1–3. Root growth of infected trees was thereby curtailed in relation to the amount of infection. The relationship of dbh to root growth follows the same curve regardless of the amount of root infection (2). In other words, rapidly growing trees, a number of years after becoming infected, displayed dbh and root system sizes that were similar to those of healthy slower growing trees. Effects of competition indices (8) and site index were applied to dbh growth as factors. Site index was set at 100 for medium-quality sites.

Estimated reduction in viability of *P. weirii* in roots was based on results from Oregon showing decrease in viability with increasing time (13) and retreat of viable mycelium from the root periphery towards the root collar over time (7). Viability reduction was calculated for root segments in each cell as a function of time since tree death, either by felling or mortality, and the relative horizontal distance of each cell from the stem base (Table 2, Equation 10). Although root diameter has not been conclusively linked to longevity of *P. weirii* in roots over periods of 5 to 11 yr (18), it was assumed that over longer periods the fungus would disappear most rapidly from the smaller, more peripheral root elements (7). Thus most rapid loss of viability would occur with increasing time after tree death and increasing distance from the root collar (Fig. 5). The viability reduction coefficient was empirically determined to produce an average reduction rate similar to those reported in Oregon.

Variation in initial mycelial distribution among stump roots (7,14, and Bloomberg, *unpublished*) was mimicked by randomly assigning one or more quadrants of stumps to be infectious. Trees lying outside infected stump quadrants were excluded from the infection process.

In summary, the model quantified the processes of root distribution in time and space, root contact, infection, mycelial spread, stem-growth reduction, mortality, inoculum viability reduction, and stump infectivity. The equations were encoded in a FORTRAN 77 program for use on a Digital Equipment Corporation VAX minicomputer.

Model testing. Three independent methods were used for testing accuracy of estimates of tree-growth reduction and mortality produced by the model. First, model results were compared with field plot measurements at a specific stand age. Second, model results were compared with those produced by RREST, the statistical spread and impact model that has been tested with satisfactory results over several years (1). Third, disease progress curves produced by the model were compared with observed disease behavior in stands of different ages and in site conditions on southern Vancouver Island.

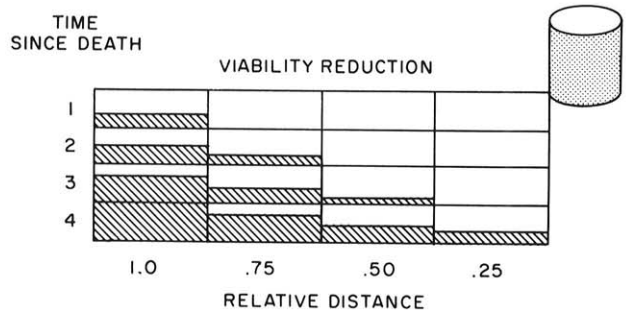

Fig. 5. Reduction of mycelial viability of *Phellinus weirii* in root elements in soil matrix cells as a function of the time since death of the tree and the relative horizontal distance from the stem base. Time is in 5-yr periods and distance is the proportion of total root system extent. Hatched portions show proportion of elements with nonviable mycelium in each cell. Viability decreases with increase in time since death and distance from stem base. Maximum reduction occurs in furthest cell at longest period since death of tree. For calculation of viability reduction in cells, see Table 2, Equation 11.

Sensitivity analyses of biological variables were used to judge the stability of the model.

Field plot data for comparison with model results comprised two approximately 1-ha stands of 60-yr-old Douglas-fir in western Oregon, containing 800–1,200 stems per hectare, with all stump and tree species, locations, diameters, and infection status recorded (16). For modeling purposes, the same diameters, coordinates, and infection status were assigned to stumps. Dbh values were assigned to trees at stand age 1 such that at age 60 they would produce the same proportions of 5-cm dbh classes as healthy trees in the field plots. Tree coordinates were assigned randomly.

The model was executed for 16 age classes (80 yr) so that comparisons with field plot data could be made up to 60 yr or later. Model results were compared with field measurements with respect to percent healthy, infected and killed stems per hectare, and basal area per hectare. Spatial distribution of infection and mortality on stem maps produced by the model were compared to distribution in the field plots. Areas of living infected trees were defined by their estimated crown projections. It was assumed that stem-growth reduction $<5\%$ would not be visually detectable in the field. Boundaries between dead, healthy, and infected tree areas were drawn on model maps through midpoints between peripheral trees of each type.

To compare the model results with RREST data, the same plot sizes (80×80 m), stand ages (1–60 yr), stump numbers (100/ha), diameters (100 cm), and coordinates were used for both models. Number of trees was set at 1,000/ha to correspond to the full stocking levels implicitly assumed in the statistical model. Areas of killed, infected, and healthy trees and the growth reduction calculated by each model were compared.

Disease progress curves generated by the model results were compared to observed disease progress in stands of various ages and on different sites on southern Vancouver Island.

Sensitivity analyses of biological variables used in the model were conducted using single or multiple infection sources in a 40×40 m plot with 1,000 stems per hectare. Rates of mycelial spread were set at 10, 20, or 30 cm/yr, representing approximately half, full, or one-and-a-half times the rate measured in experiments (17); the coefficient for fungus viability was set to half, equal to, or

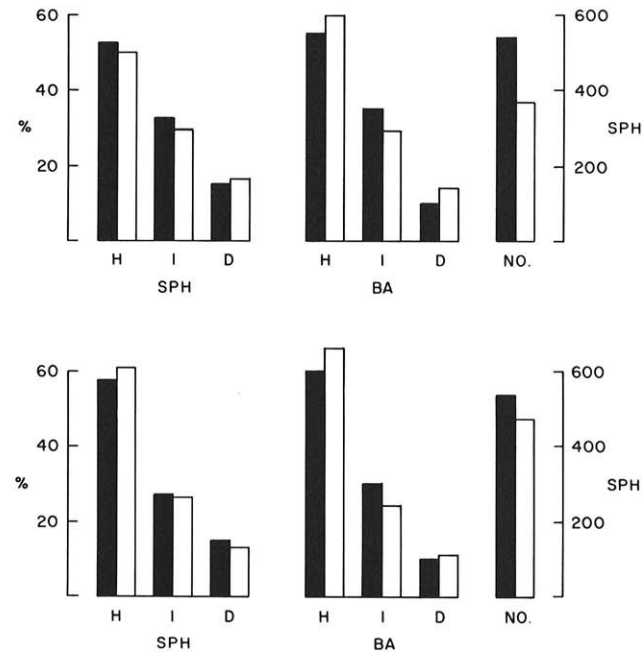

Fig. 6. Comparison of modeling estimates of laminated root rot (*Phellinus weirii*) effects in plots of Douglas-fir with recorded effects in field plots (16). **Top,** Field plot 3; **bottom,** field plot 4. SPH = No. stems per hectare; BA = tree basal area per hectare; H = percent healthy; I = infected living; D = infected dead; NO = total number of trees per hectare. Solid bars = field record results; open bars = modeling estimates.

one-and-a-half times the rate required to reduce viability recorded in Oregon (7); and site index was set at 50, 100, or 150 (10), representing poor-, medium-, or high-quality sites.

Effects of stand conditions were examined by varying the numbers of infected stumps from 25 to 75/ha, representing low, moderate, and high inoculum levels, in combination with stump infection levels of 25, 50, and 75% (one, two, or three infectious quadrants, respectively). Number of trees per hectare was set at 1,000, stump diameters at 50 cm, and plot size at 40 × 40 m.

RESULTS AND DISCUSSION

Comparison of model results with field measurements in the Oregon plots showed general agreement for percent healthy, infected, and dead stems per hectare, and basal area per hectare (Fig. 6). Total stems per hectare were somewhat fewer in the model mainly because the initial densities were based on field plot records that excluded trees <15-cm dbh. These levels almost certainly underestimated stand densities at the start of growth by the amount of early suppression mortality unrelated to root rot (10).

Spatial pattern of infection on stem maps produced by the model approximated that of the field plots with respect to the main areas of healthy and killed trees (Figs. 7 and 8). Areas containing living infected trees were more fragmented in field plots than on the model maps. Difficulty in equating visible symptoms in individual trees to percent growth reduction calculated by the model prevented a definition of infection boundaries as exact as was possible in the field.

Comparison of the model results with RREST results showed similar distributions of mortality, living infected, and healthy areas at age 60 (Fig. 9). Boundaries between the three types of areas were more regular in the statistical model because it did not depend on tree distribution and assumed isodiametric expansion of infection centers. Growth reduction calculated by the model for the stand as a whole and in infection centers alone was 33.8 and 55.3%, respectively, compared to 31.9 and 44.6% for the statistical model.

Disease progress curves produced by the model showed realistic trends as observed from second-growth Douglas-fir stands on southern Vancouver Island. The initial mortality at 5 to 15 yr (Fig. 10) was interpreted as the result of planting seedlings directly on stump roots infected by *P. weirii* (Bloomberg, *unpublished*). The stable mortality from 15 to 40 yr reflected the lack of root contact among trees due to their small size. No further dying occurred until about age 40 when the root systems closed and root contacts increased. At this age, stand damage became conspicuous and continued to rotation age (100 yr) (4).

Sensitivity analyses showed that increasing linear mycelial growth rates markedly increased tree mortality at stand age 60 under the conditions set, i.e., a single infection source placed

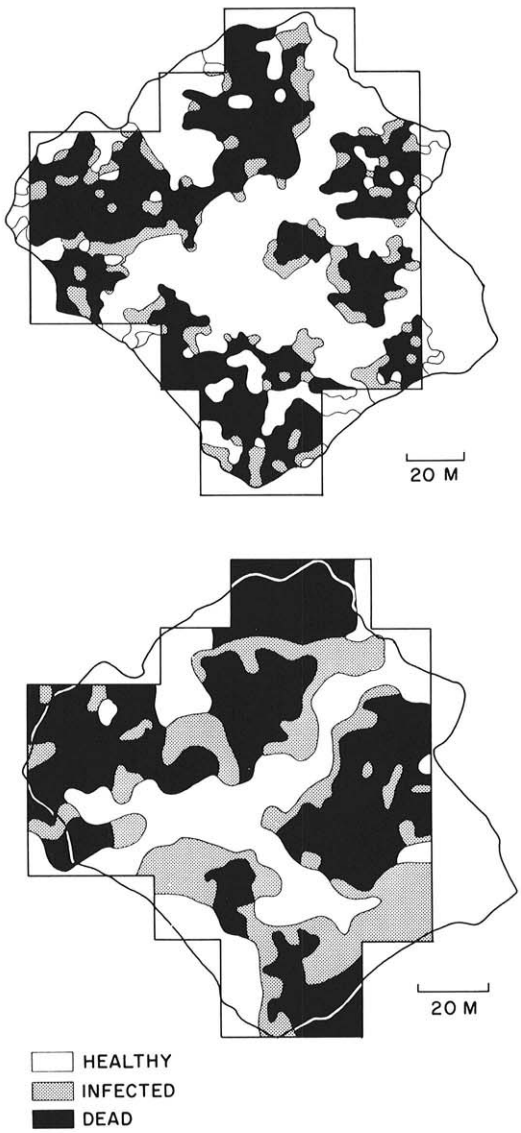

Fig. 7. Comparison of modeling estimates of laminated root rot (*Phellinus weirii*) spatial distribution in a plot of Douglas-fir with recorded distribution in a field plot. **Top,** Field plot 3 (16); **bottom,** model results. Scale of maps slightly different because of fixed printer page size.

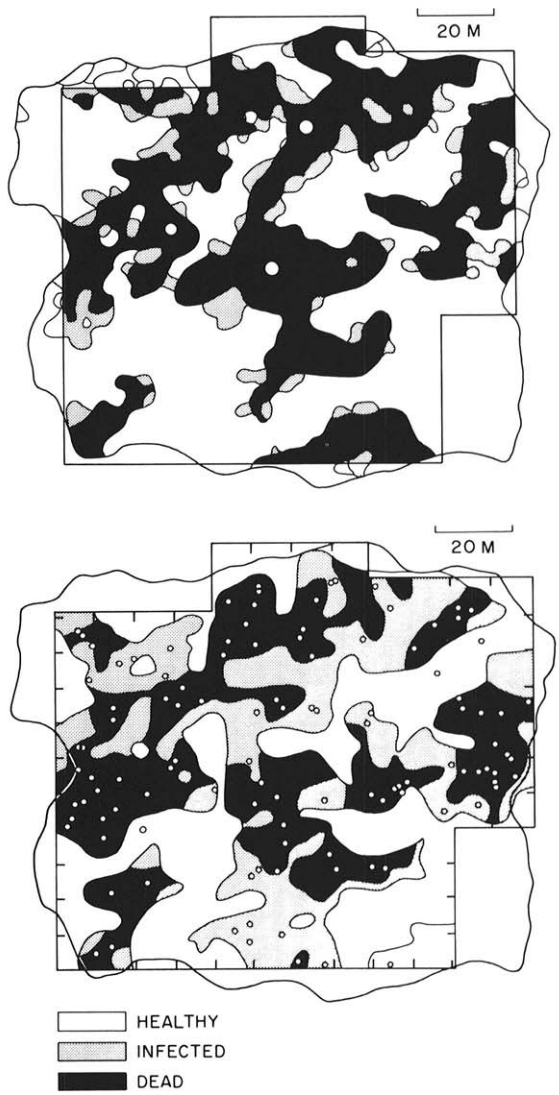

Fig. 8. Comparison as for Fig. 7 but with positions of infected stumps also shown (small open circles). **Top,** Field plot 4 (16); **bottom,** model results.

centrally in a plot (Fig. 11). However, this effect was not so evident when multiple infection sources were used because root systems could then be infected at numerous points, lessening the importance of mycelial spread. Inoculum viability reduction had only a weak effect on tree mortality. This variable had most effect in the initial infection phase, i.e., from stump roots. Later on, the importance of viability was reduced when intertree infection became the dominant means of mycelial spread. Increased site index markedly increased mortality due to more rapid tree growth accompanied by larger root systems and more frequent root contact.

Mortality increased with both increasing number of infected stumps per hectare and stump infectivity (Fig. 12) as would be expected from field observations.

Further investigations will use the model to estimate the effects of stand densities, species composition, inoculum levels, and site quality on tree growth and mortality. The effects of tree removal by spacing, thinning, and sanitation will be estimated. The objective is to recommend broad guidelines for silvicultural treatment of

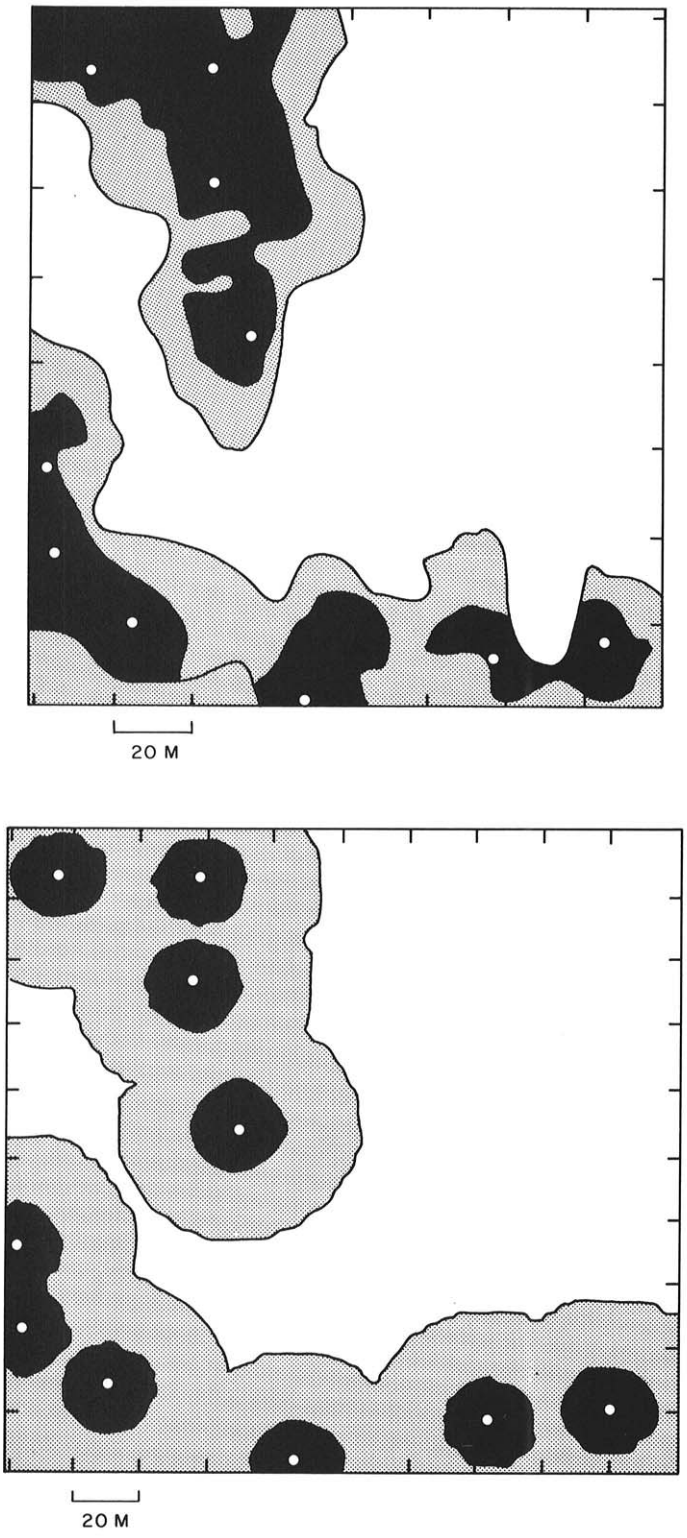

Fig. 9. Comparison of model estimates of laminated root rot (*Phellinus weirii*) effects at stand age 60 in a plot of Douglas-fir with those from a statistically based spread and impact model. **Top,** Model described in this report; **bottom,** statistically based model. Small open circles = positions of stumps of same size and at same locations in both models; solid areas = killed trees; hatched areas = infected trees; blank areas = healthy trees.

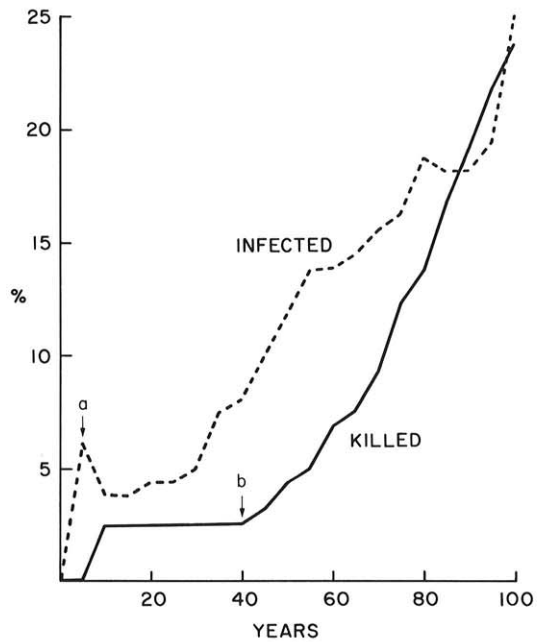

Fig. 10. Disease progress curve produced by model showing trends of laminated root rot (*Phellinus weirii*) effects on a Douglas-fir stand over time. **a,** Initial infection of seedlings planted directly in contact with diseased roots; **b,** start of sustained mortality due to increased root contacts among trees.

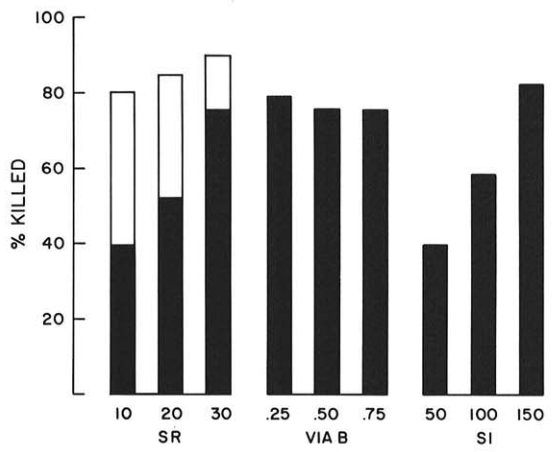

Fig. 11. Results of a sensitivity analysis of three variables used in modeling laminated root rot (*Phellinus weirii*) of Douglas-fir. Solid bar = single infection source; open bar = multiple infection sources. **Left,** Mycelium spread rates (SR) set at 10, 20, or 30 cm/year; **middle,** mycelium viability reduction rates (VIAB) of 25, 50, or 75%; **right,** site index set (SI) at 50, 100, or 150, corresponding to poor, medium, and good. Vertical axis is percent tree mortality at 60 yr.

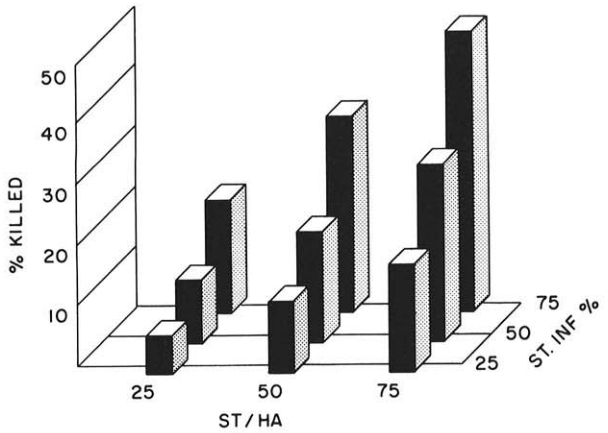

Fig. 12. Effect of using different numbers per hectare (ST/HA) and infection status (STINF%) of stumps in modeling laminated root rot (*Phellinus weirii*) in a Douglas-fir stand. Results are at stand age 60.

stands infected by *P. weirii* that are based on the best available information on the epidemiology of the disease. The infection subroutines of the model have been incorporated in the Douglas-fir stand-growth model TASS (11), and results from the combined models will be tested against field plot data. If the results are satisfactory, it may be possible to develop yield tables for infected stands.

LITERATURE CITED

1. Bloomberg, W. J. 1983. A ground-survey method for estimating loss caused by *Phellinus weirii* root rot. III. Simulation of disease spread and impact. Can. For. Serv. BC-R-7. Ottawa, Ont., Can. 24 pp.
2. Bloomberg, W. J., and Hall, A. A. 1986. Effects of laminated root rot on relationships between stem growth and root-system size, morphology, and spatial distribution in Douglas-fir. For. Sci. 32:202-219.
3. Bloomberg, W. J., and Reynolds, G. 1982. Factors affecting transfer and spread of *Phellinus weirii* mycelium in roots of second-growth Douglas-fir. Can. J. For. Res. 12:424-427.
4. Bloomberg, W. J., and Reynolds, G. 1985. Growth loss and mortality in laminated root rot infection centers in second-growth Douglas-fir on Vancouver Island. For. Sci. 31:497-508.
5. Br. Columbia Minist. For. 1984. Page 45 in: Annual Report. Queen's Printer of British Columbia, Victoria, B.C.
6. Childs, T. W., and Shea, K. R. 1967. Annual losses from disease in Pacific Northwest forests. U.S. For. Serv. Res. Bull. PNW-20. Pac. Northwest For. Range Exp. Stn., Portland, OR. 19 pp.
7. Hansen, E. M. 1979. Survival of *Phellinus weirii* in Douglas-fir stumps after logging. Can. J. For. Res. 9:484-488.
8. Hegyi, F. 1973. A simulation model for managing jack pine stands. Pages 74–90 in: Growth Models for Tree and Stand Simulation. J. Fries, ed. Proc. Internat. Union For. Res. Organizations Working Party S4.01-4. Vancouver, B.C., Can.
9. McMinn, R. G. 1963. Characteristics of Douglas-fir root systems. Can. J. Bot. 41:105-122.
10. Mitchell, K. J. 1985. Managed stand yield tables for coastal Douglas-fir: initial density and precommercial thinning. Res. Branch Land Manage. Rep. 31. B.C. Minist. For., 69 pp. Queen's Printer of British Columbia, Victoria, B.C.
11. Mitchell, K. J., and Bloomberg, W. J. 1986. Expanding concepts of growth and yield modeling to disease impacts and forest products. Pages 3-18 in: Proc. Can. For. Serv. 2nd Modeling or Workshop. Victoria, B.C., Can.
12. Monro, D. D. 1974. Forest growth models—a prognosis. Pages 151-154 in: Growth Models for Tree and Stand Simulation. J. Fries, ed. Res. Note 30. Dep. For. Yield Res., Inst. Silogsproduktion, Stockholm, Sweden.
13. Nelson, E. E. 1967. Factors affecting survival of *Poria weirii* in small buried cubes of Douglas-fir heartwood. For. Sci. 13:78-84.
14. Reynolds, K. M., and Bloomberg, W. J. 1982. Estimating probability of intertree contact in second-growth Douglas-fir. Can. J. For. Res. 12:493-498.
15. Thies, W. G. 1983. Determination of growth reduction in Douglas-fir infected by *Phellinus weirii*. For. Sci. 29:305-313.
16. Tkacz, B. M. 1979. Comparison of *Phellinus weirii* root rot damage in a 60-year-old Douglas-fir (*Pseudotsuga menziesii*) stand with the damage in the preceding old-growth stand. Ph.D. thesis. Oregon State University, Corvallis. 114 pp.
17. Wallis, G. W., and Reynolds, G. 1962. Inoculation of Douglas-fir roots with *Poria weirii*. Can. J. Bot. 40:637-645.
18. Wallis, G. W., and Reynolds, G. 1965. Initiation and spread of *Poria weirii* root rot of Douglas-fir. Can. J. Bot. 43:1-9.